Applied Geography 101 (2018) 56–67

Contents lists available at ScienceDirect

Applied Geography

journal homepage: www.elsevier.com/locate/apgeog

Liberia's coastal erosion vulnerability and LULC change analysis: Post-civil war and Ebola epidemic

J.L. Awange[a], A. Saleem[a,*], S.S. Konneh[a], R.M. Goncalves[b], J.B.K. Kiema[c], K.X. Hu[a]

[a] Discipline of Spatial Sciences, School of Earth and Planetary Sciences, Curtin University, Perth, Australia

[b] Department of Cartographic Engineering, Geodetic Science and Technology of Geoinformation Post Graduation Program, Federal University of Pernambuco (UFPE), Recife, PE, Brazil

[c] Regional Centre for Mapping of Resources for Development, Nairobi, Kenya

ARTICLE INFO

Keywords:
LULC changes
Coastal vulnerability
Erosion
Supervised classification
Landsat
Sentinel-2
Liberia

ABSTRACT

In most developing countries, data for coastal change and vulnerability assessment is hard to come by due, e.g., to data inaccessibility or incomplete dataset. In some countries, e.g., Liberia, a country that was ravaged by civil war and Ebola epidemic, such extraneous factors prevent direct observations, i.e., "boots on the ground". This study examines temporal changes in land use/land cover (LULC), coastline changes, and coastal vulnerability to erosion and their effects on Liberia over a period of 29 years (1986–2015). The results from the post-classification change detection analysis using Landsat data (validated by moderate resolution Sentinel-2 product) show that bare land and sediment classes decreased over the entire study period by 5.07% and 0.06%, respectively. Water, vegetation, and residential classes are found to have increased during the 29 years of evaluation by 0.41%, 3.29% and 1.43%, respectively. Vegetation cover during the post-civil war era (2002–2015), however, reduced by about 0.31%. Furthermore, the results for the coastal analysis indicate more erosion during the period 1998–2002, i.e., the post-civil war period. The results also show an increase in residential areas possibly due to population growth, especially in the most populated areas such as Monrovia, the capital city.

1. Introduction

Liberia's coastal zone (Fig. 1) is particularly vulnerable to among others climate change induced erosion (UNDP, 2015), which increased in recent years leading to the displacement of many people. Coastal erosions affected local businesses and infrastructure such as medical centres, roads, markets and livelihood equipments along the coast, e.g., West Point, a densely populated slum in Monrovia, the capital city of Liberia (Global Environmental Facility, 2010; Graham, 2014; MacDougall, 2016; Werrell & Femia, 2014; Williams, 2016). In addition to the increase in displaced population, increased flooding in Liberia is also negatively impacting the country's agricultural sector (Global Environmental Facility, 2010), further putting more pressure on the already struggling economy. In June 2007, for example, flash flood in Monrovia left about 300 people displaced (UNDP, 2015). Increase in erosion instances are largely due to several factors that include but not limited to Liberia's inability to adapt to climate change (UNDP, 2015; USAID, 2012). There is limited understanding of the causes of coastline changes and erosion among decision making authorities in Liberia. Few agencies that collect data on the coast and climatic condition in Liberia lack coordination among themselves, working independently with no combined database and management systems (UNDP, 2015).

Liberia has had its share of calamities in the last three decades. First, it was ravaged by the 14 years civil war that left about 250,000 people dead and many thousand displaced (John, 2017). Second, in 2014, the country was faced by the Ebola virus epidemic that left over 2484 people dead (CDC, 2017). The efforts to minimise the spread of the virus limited people's movement both within Liberia and across the borders. This in turn led to a further financial constraint in the country as trading activities were limited. People in self-employment were typically more affected by the spread of the virus (The World Bank, 2016). These calamities have negatively impacted the economy of Liberia and its capacity to adapt to climate change and coastal erosion challenges. Due to the effects of the civil war and the 2014 Ebola crisis, there is a lack of financial resources, shortage of scientific data, and difficulties to manage the coast considering coastal erosion problems and climate changes over Liberia (USAID, 2012). Unless these issues are addressed properly, erosion will probably continue to create more problems for Liberia.

Monitoring Liberia's coastline and its rate of change, therefore, is

* Corresponding author.
E-mail address: ashty.saleem@curtin.edu.au (A. Saleem).

https://doi.org/10.1016/j.apgeog.2018.10.007
Received 22 April 2018; Received in revised form 19 August 2018; Accepted 21 October 2018
Available online 14 November 2018

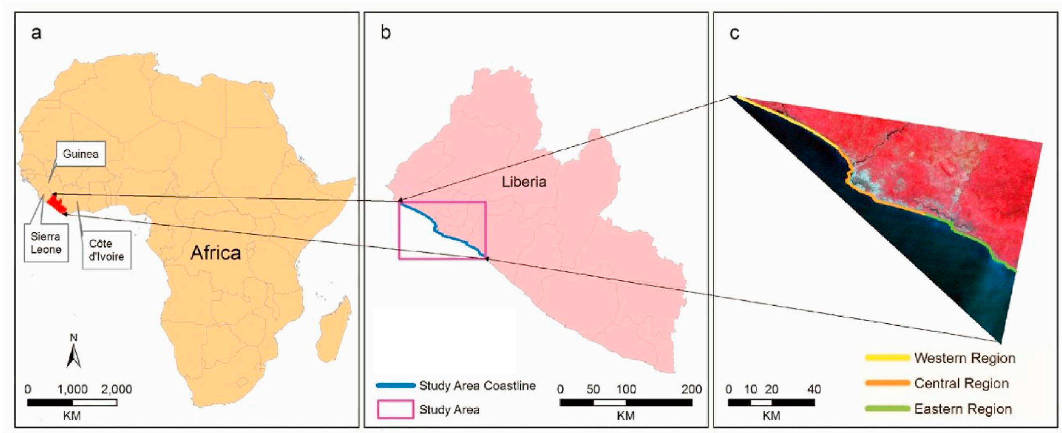

Fig. 1. (a) The Geographical location of Liberia within Africa, (b) a zoomed map of Liberia showing the study area, and (c), the chosen study area with the three study regions represented by three different colours. (For interpretation of the references to colour in this figure legend, the reader is referred to the Web version of this article.)

paramount and strategically important for environmental protection and sustainability (Pardo-Pascual, Almonacid-Caballer, Ruiz, & Palomar-Vzquez, 2012; Poornima & Chinthaparthi, 2014). Such studies provide information that can enable coastal management authorities to take corrective measures to minimise the effects of coastal changes (Pardo-Pascual et al., 2012). Coastline monitoring and change detection studies are economically very important and have therefore attracted a large number of researches globally (see, e.g., Goncalves, Awange, Krueger, Heck, & Coelho 2012). Traditionally, the "boots on the ground" coastline mapping surveys is preferred since it provides a number of important benefits such as (Goncalves & Awange, 2017); (i) for very small project sites, the total acquisition cost can actually be lower using ground-based methods than for airborne methods, (ii) ground-based coastline surveys, e.g., Global Navigation Satellite System (GNSS; e.g., wange, 2012, 2018; Goncalves, Awange, & Krueger, 2012) typically provide the highest accuracy when compared with medium resolution satellite images such as Landsat, as well as the fact that detailed knowledge obtained by ground-based surveys can provide reference data for calibrating and validating airborne and space-borne shoreline mapping techniques, and (iii), when coastline data with high temporal resolution (i.e., short repeat survey periods) are needed, ground-based methods may be the best option.

Even with the advantages of ground-based methods listed above, coastline monitoring are highly labour intensive and expensive and out of reach for most developing countries such as Liberia (Alesheikh, Ghorbanali, & Nouri, 2007; Appeaning Addo, Walkden, & Mills, 2008). Moreover, for Liberia, war and Ebola crisis practically made ground-based collection of useful baseline coastline monitoring data practically impossible and prevented exploitation of such data for coastal change and vulnerability analysis. As a result, the use of modern remote sensing data sources, e.g., Landsat and ASTER, and GIS analysis provide efficient alternative platforms for coastline monitoring for such countries (see e.g., Goncalves & Awange, 2017; Yu, Hu, Muller-Karger, Lu, & Soto, 2011). These data sources allow analysis of areas with limited accessibility in a sufficiently accurate and efficient manner, see e.g., (Jayson-Quashigah, Addo, & Kodzo, 2013). Other airborne approaches that have found use and proven to be effective methods for coastline mapping globally include, e.g., airborne Lidar, photogrammetry techniques, and other satellite images (see e.g., Graham, 2014; Parrish, Sault, White, & Sellars, 2005; Smith, 1981, p. 486).

Against this background, this study aims to investigate the possibility of using freely available remotely sensed Landsat products within a GIS platform to monitor LULC and coastline changes over Liberia. To achieve this, the study (i) determines changes in different LULC classes (vegetation, sand dunes, water bodies, residential areas and bare land) and investigates their relationship to changes along the coast, (ii) investigates and estimates the rate of erosion and accretion along the coast during the period 1986–2015, (iii) investigates the changes in sea-level rise and its relation to the coastal erosion, and (iv), carries out a coastal erosion vulnerability assessment.

Assessing and analysing the vulnerability of the coast to erosion is important for city planning and disaster relief management (Sousa, Siegle, & Tessler, 2013). Different studies have adopted different approaches to assess coastal vulnerability to erosion. Bryan, Harvey, Belperio, and Bourman (2001) uses distributed coastal process modelling approach to assess vulnerability level of False Bay in South Africa and Northern Spencer Gulf in Southern Australia. Using this approach, Bryan et al. (2001) modelled the spatial distribution of four environmental parameters (elevation, exposure, slope and aspect derived from Digital Elevation Model (DEM) data), which can influence coastal inundation and erosion. Sousa et al. (2013) and Pendleton, Thieler, and Williams (2005) developed coastal vulnerability indices using coastal and inland erosion indicators (beach morphology, shoreline positions, dune field configurations, wave exposure, rivers, terrain elevations, vegetation, coastal engineering structures and build-up environments). Our contribution assesses coastal erosion vulnerability using different variables based on available information on the Liberian coast, i.e., annual coastline shifts, coastal slopes, vegetation and residential areas.

The remainder of the study is organised as follows. In section 2, Liberia's coast is presented while section 3 provides the data and methods employed. Section 4 discusses the results and the study is concluded in section 5.

2. Liberia's coast

Liberia (4°20′ - 8°30′ N; 7°18′ - 11°20′ W, see Fig. 1) is a West African nation bordered by Sierra Leone to the west, Guinea to the north, Côte d'Ivoire (Ivory Coast) to the east, the Atlantic Ocean to the south, and covers an area of about 111,369 km^2 (LISGIS, 2014), with an estimated population of over 4.5 million people (The World Bank, 2016). Its coastline of about 559 km is home to about 58% of the Liberian population (Nicholls & Cazenave, 2010; USAID, 2012), a majority of whom live in low-lying lands, with houses poorly constructed close to the beaches (UN DESA, 2015). Geographical features along Liberia's coast include lagoons, sandbars and mangrove swamps. The topography of Liberia is largely flat with the highest point being the top of Mount Wuteve (1380 m above mean sea level). The area of interest for the present study covers about 180 km of Liberia's coast (Fig. 1).

Liberia's humid and tropical climate is characterised by the proximity of the country to Atlantic Ocean (LISGIS, 2014), and has little

variation in temperature throughout the year. The average monthly temperature ranges from 24.2°C to 27°C while its two rainy seasons run from April to October and the dry season starts from the beginning of November and ends in March (Wiles, 2005). More rainfall occurs in areas closer to the coast with monthly average rainfall ranging from 22.1 mm in January to 383.6 mm in September (LISGIS, 2014).

3. Data and methods

3.1. Landsat and Sentinel-2 data

The multi-spectral Landsat and Sentinel-2 data have a wide range of spectrum bands that includes, visible to Near-Infrared (VNIR) and shortwave Infrared (SWIR) wavelengths. Landsat satellite system collects multi-spectral images that are useful for monitoring and understanding human activities, e.g., detecting, measuring and highlighting changes in landscape patterns over time including those of coastal studies (USGS, 2015). Since changes in the landscape are dynamic, these imagery can be used to study and capture extent of changes at large scale within short time frames and at no cost since the images are free. Without remotely sensed data, the task of capturing and mapping changes in landscape would be much more difficult and time consuming. The imagery from Landsat platform, which can be accessed freely from USGS website (https://earthexplorer.usgs.gov/) are powerful data source providing accurate and timely spatial information on changes in the Earth's landscape. Because of its long-term digital archive since 1972, it has been used in many land use and land cover change studies over different parts of the world, see e.g., Jensen, Rutchey, Koch, and Narumalani (1995).

Over the past 46 years, there have been numerous studies that have used Landsat imagery for agriculture forecasting and management (production and conservation) (see, e.g., Kauth, Lambeck, Richardson, Thomas, & Pentland, 1979; Stow, Tinney & Estes, 1980; Peterson and Aunap, 1988; González-Sanpedro et al., 2008). Its other applications are reported in (see, e.g., Cihlar, 2000; Jusoff & Senthavy, 2003; Porter-Bolland, Ellis & Gholz, 2007; Dewan & Yamaguchi, 2009; Kesgin & Nurlu, 2009; Vittek, Brink, Donnay, Simonetti, & Descle, 2014; Yadav, Kapoor, & Sarma, 2012; Otukei & Blaschke, 2010; Moran, 2010). Landsat data, therefore, are important when there are no other accurate way of mapping and detecting changes due to cost, time, and access constraints. Landsat datasets obtained from the USGS are Level 1 products, which have been corrected for terrain effects, calibrated radiometrically, and geographically georeferenced (USGS, 2015). This study uses multitemporal Landsat images to analyse and detect changes in different LULC in Liberia from 1986 to 2015, a period covering both the time of civil war and the post-war. Coastlines are extracted and areas of erosion and accretion for the Liberian coast determined and evaluated. Since a single Landsat scene covers the full extent of the study area, four scenes are required for the coverage of four years (1986, 1998, 2002 and 2015) considered in this study. Due to lack of available adequate satellite scenes, variations existed in the intervals of the four periods evaluated for this study.

To validate the used Landsat images whose spatial resolution is 30 m, the Sentinel-2 (MSI) with 10 m spatial resolution, officially launched by ESA on June 23, 2015, with a 5-day temporal resolution or repeat cycle (ESA, 2017) was employed. The corporation between ESA and the USGS provides Sentinel-2 (MSI) data in Level-1C product to end users and can be accessed from the USGS website and the official website of the Copernicus Open Access Hub for the European Space Agency (ESA) (https://scihub.copernicus.eu/). Sentinel-2 data has been processed by ESA and USGS to include radiometric and geometric corrections along with ortho-rectification to generate highly accurate geo-located products for researchers (Drusch et al., 2012). The information on the Landsat scenes and Sentinel-2 used for this research, are summarised in Table 1.

The pre-processing applied on the four Landsat images are the atmospheric corrections using Dark Object Subtraction (DOS) method, image co-registration, and image sub-setting using Area Of Interest (AOI) vector file. DOS method has been recommended, e.g., by Song, Woodcock, Seto, Lenney, and Macomber (2001) as a preferable method that is strictly based on information from the images (Gilmore, Saleem, & Dewan, 2015). For the pre-processing step, Sentinel-2 MSI 2015 images were used as a reference to register Landsat images considering Universal Traverse Mercator (UTM) grid zone 29°N (Liberias map grid) using ENVI software. During image registration process, well distributed Ground Control Points (GCPs) represented by permanent features such as bridges and road intersections are selected (a minimum of 20 for each image). Using a first order polynomial fit, the registration process yielded a maximum Root Mean Square Error (RMSE) of 0.5 pixels (i.e., 15 m) for each scene. Each of the four Landsat scenes was finally clipped with the area of interest (AOI) shapefile.

The supervised classification method with Maximum Likelihood Classification (MLC) is employed to create five different LULC classes for Landsat images, i.e., water, vegetation, bare land, sediment and residential. Water represents all the water pixels present in the study area including ocean, rivers, lakes and lagoons. Vegetation class represents permanent crops, forests, and mangroves. Sediment class represents sand dunes or beach areas while residential and bare land classes represent urban areas and barren lands, respectively. Using the ArcGIS software, training samples for each Landsat image and for each land use/cover classes are generated through manual digitisation. These classes are then labelled according to the land cover class category they represent. Signature files for each Landsat image are then generated and used as input for Maximum Likelihood Classification. The MLC method tends to overclassify especially with large covariance matrix (Rawat & Kumar, 2015). This method is one of the most widely used classification method in the remote sensing field (see, e.g., Abd EI-Kawy et al., 2011; El-Hattab, 2016; Misra & Balaji, 2015; Rawat & Kumar, 2015). It not only considers most variables but also takes into consideration the variability between classes by using covariance matrix (Mather & Koch, 2011).

3.2. Data validation and change detection

To quantify the level of uncertainty that may be present in the LULC maps, accuracy assessment is performed to evaluate the quality of the image classification process. In view of this, representative ground truth data (reference dataset) is created by generating 750 random points in ArcGIS. All the random points are overlayed on the 2015 Sentinel-2 MSI image (10 m spatial resolution) and 500 points (100 for each class) attributed with correct LULC classes and same codes representing them in classified images. Because of lack of the reference data to evaluate the results for each year individually, the unchanged areas are highlighted among all Landsat images and accuracy assessment process performed. The reference dataset is combined with the unchanged areas for all evaluated years to form a confusion matrix and used to compute different values of user's accuracy, producer's accuracy, overall accuracy, and kappa coefficient.

There are many different methods of change detection analysis, which have been used for LULC change studies, including image differencing, vegetation index differencing, principal component analysis (PCA) and post classification comparison (e.g., Abd EI-Kawy et al., 2011; El-Hattab, 2016). For this study, post-classification “cross tabulation” technique is employed (see, e.g., Saleem, Corner, & Awange, 2018). With this method, the size and distribution of areas that changed and those that remained stable throughout the study period are derived, also the rate of changes by other classes can be derived for each period generated during this process (El-Hattab, 2016).

Table 1
Landsat and Sentinel-2 images used in the study. Landsat images have been used for the analysis while Sentinel-2 are used as reference data for the validation.

No. of images	Platform/Sensor	Acquisition date	Spatial resolution (m)	Cloud cover (%)
1	Landsat 5 TM	21 Jan 1986	30	0.0
1	Landsat 5 TM	23 Feb 1998	30	29.0
1	Landsat 7 ETM+	27 Dec 2002	30	4.0
1	Landsat 8 LDCM	23 Dec 2015	30	3.2
4	Sentinel-2 MSI	26 Dec 2015	10	0.0

3.3. Coastline extraction

The coastline from each Landsat scene is extracted using on-screen manual digitisation technique with constant scale of 1:5000 and with a single operator. This technique has been proven to be ideal for rivers and coastline extraction by studies such as Dewan et al. (2017); Salghuna and Bharathvaj (2015), respectively. Instantaneous water lines are used as proxies for coastlines. The study area is divided into three sub-regions; western, central, and eastern regions (see Fig. 1c). Polylines derived through this method are superimposed onto a reference scene to derive erosion and accretion for the periods between 1986 and each of other years 1998, 2002 and 2015. Because the linear length of each of these regions is about 50 km, it is impossible to calculate the areas of erosion and accretion from overlaid coastlines. For this reason, a Sliver Polygons dataset is created using auto-complete tool during editing session in ArcGIS. Areas of erosion and accretion are then calculated for these three sub-regions of the study by taking the spatial union of two successive polylines as suggested, e.g., by Dewan et al. (2017).

For the coastline shift, as in Dewan et al. (2017), orthogonal profiles are generated at an interval of 500 m for the 1986 coastline dataset as baseline using the transect tools in ArcGIS. Because the 1986 coastline shapefile is the most historic coastline among other extracted years, it is used as the baseline (reference coastline). The profiles are visually inspected to ensure that they are all orthogonal to the baseline year. Coastline change of each profile is then calculated for the different periods by comparing two extracted coastline areas. The orthogonal profiles and polygons for erosion and accretion created earlier are intersected. The erosion and accretion information from the polygon are transferred to the orthogonal profiles. The lengths of the orthogonal profiles are calculated to display coastlines shift over the years.

3.4. Satellite altimetry data

Multi altimetry satellite gridded sea level surface data covering a period of twenty-two years (1993–2015) acquired from Copernicus Marine Environment Monitoring Service (CMEMS) is used to assess sea level changes. The satellite altimetry data (available on http://marine.copernicus.eu) used here is produced by SL-TAS multi-mission altimetry processing system. The data was processed from all altimetry mission, including HY2, Saral/AltiKa, Cryosat-2, Jason-2, Jason-1, T/P, ENVISAT, GFO, ERS1/2. The study period could not be fully covered in sea surface variability assessment as tide gauge data could not be obtained to compensate for the period not recorded by satellite altimetry as done, e.g., in Awange et al. (2013).

Multi-mission altimetry data acquired for assessing sea level changes have been pre-processed by the data proprietor. Multi-mission cross-calibration, interpolation at crossover locations and dates, repeat-tract analysis, and data cross-validation are some of the processing steps performed by the data proprietor to obtain gridded sea level anomaly (SLA). The gridded mean sea level data, obtained in Network Common Data Format (NetCDF) format is processed in MATLAB R2016a to plot the time series of daily sea surface variability for the evaluated years. MATLAB's polyfit function is used to fit the first order polynomial, the line of best fit. To find out if there is a relationship between erosion and each of the LULC, and coastline movement, Pearsons *r* correlation coefficient is computed.

3.5. Trend analysis

The slope value for sea level changes and the annual coastline rate of shifting over the study period (1986–2015) are tested for statistical similarity using the Welch's *t*-test. Pre-dominantly, Student *t*-test is used for testing statistical significance between two different means or slopes. Student *t*-test assumes that samples being tested have equal variance and that the data follows a normal distribution (Ruxton, 2006). Because of the assumption of equal variance, the student *t*-test is not used in this study rather, the Welch's *t*-test (unequal variances *t*-test), which is proven to be a better alternative to student *t*-test (Ruxton, 2006) is used instead. This test does not assume the equality of variances and even when the variances are equal, the Welchs *t*-test is still as powerful as the Student *t*-test (Moser, Stevens, & Watts, 1989; Ruxton, 2006). The implementation of this test primarily requires information on the standard deviation, mean and sample sizes for the two data being tested. Since the coastline movement is computed by comparing two sequential images, standard deviation and mean values are computed using the values of shifting at each orthogonal profile location.

Let a_1 and a_2 be the slopes of coastline shifting and average sea level changes, respectively. The null and alternative hypothesis are expressed as:

$$H_0\colon a_1 = a_2,$$

$$H_1\colon a_1 \neq a_2,$$

where H_0 is the null hypothesis inferring that a_1 is statistically equal to a_2, and the alternative hypothesis H_1 infers that the two slopes are not equal. Let n_1 and n_2 be the sample sizes for coastline shift and sea surface changes, respectively, and s_1 and s_2 be the standard deviations of a_1 and a_2, respectively. The statistic (t') of the Welch's *t*-test (unequal variance *t*-test) is represented by (Ruxton, 2006):

$$t' = \frac{a_1 - a_2}{\sqrt{\frac{s_1^2}{n_1} + \frac{s_2^2}{n_2}}}, \tag{1}$$

and the degree of freedom (v) given by:

$$v = \frac{\frac{1}{n_1} + \frac{u}{n_2}^2}{\frac{1}{n_1^2(n_1 - 1)} + \frac{u^2}{n_2^2(n_2 - 1)}}, \tag{2}$$

where

$$u = \frac{s_2^2}{s_1^2}. \tag{3}$$

The t'-statistic is tested against the critical *t*-value using the degree of freedom and the 0.05 significant level. If the $t'<$ *t*-critical, the null hypothesis is accepted otherwise the null hypothesis is rejected. In the instance that the null hypothesis is accepted, it can be inferred that the slopes are statistically equal, and therefore the sea level rise and coastline shifting are statistically related.

3.6. Coastal erosion vulnerability assessment

For each five indicators (accretion, erosion, residential, vegetation and coastal slope) used during the evaluation, different vulnerability classes are defined based on some of the coastline vulnerability assessment literature. For annual coastline shifting variable, vulnerability threshold values employed by Mendonça, Gonclaves, Awange, Silva, and Gregorio (2014) are adopted. Vegetation and residential variables are obtained from the LULC changes, where they show a positive relationship with observed coastal erosion. For that reason, vulnerability threshold set for them are as follow: negative percentage change (decline) of the total area during each period is considered to be very highly vulnerable. More than 0 but less than 0.5% is highly vulnerable. Greater than 0.5 but less than 0.75% is considered moderate. Between 0.75 and 1% is considered low vulnerability and more than 1% is considered very low vulnerability. The coastal slope is derived from Digital Elevation Model (DEM) data extending 1 km landwards. The DEM (SRTM 90 m resolution) is obtained from USGS's earth explorer website. As in Pendleton et al. (2005), slopes of more than 14.7% are considered very low, between 10.9 and 14.69 are low, between 7.75 and 10.89 are moderate. High vulnerable areas have slopes between 4.60 and 7.74 while less than 4.59 are considered as very highly vulnerable areas. These thresholds are based on the assumptions that low slope coastal areas are likely to be eroded faster than steeper areas (Pendleton et al., 2005).

After defining the levels of vulnerability based on individual indicators, vulnerability level of each of the study areas is determined by considering the dominant level of vulnerability in the specific region. The overall data and methods that have been employed in this study are summarised in Fig. 2.

4. Results and discussion

4.1. LULC maps and accuracy assessment

The results of the accuracy assessment for the unchanged areas using confusion matrix for all Landsat scenes are presented in Table 2 where the overall accuracy and kappa coefficient are 86% and 0.82, respectively. As for the accuracy among the individual classes, user's accuracy ranges from 78% to 98% while the producer's accuracy ranges from 80% to 90%. The accuracy assessment results produced here satisfy the accuracy standards suggested by Anderson (1976) for LULC mapping studies using Landsat data.

The spatial pattern and area statistics of the LULC categories (classes) for all classified images are shown in Fig. 3 and Table 3, where the dominant land cover classes for the classified images are vegetation, followed by water and bare land. The vegetation and water body categories show the most stable land use/cover types during the evaluated time span of 29 years.

The areas of classified images and their change detection analysis statistics are shown in Table 3, where the results show the period 1986–1998 to have some minor increase in vegetation (1.09%) and a decrease in bare land by 1.05%. However, significant changes in terms of increase are detected in the second period 1998–2002 for vegetation and residential by 2.51% and 1.24%, respectively. Meanwhile, bare land noticeably decreased by 3.67%. In general, vegetation areas increased from 59.4% to 60.5% at the expense of decrease in other classes. As for water and sediment classes over the same period (1998–2002), they can be regarded as stable as the amount of changes are not significant (Table 3). In the third period (2002–2015), the negative trends for bare land, sediment and vegetation, could most likely be related to coastal erosion and sea level rise (UNEP, 2004; Wiles, 2005), while the increase in residential and water areas could be related to population increase (UN DESA, 2015) and to erosion (Wiles, 2005), respectively. Finally, the fourth period (1986–2015) gives an overview of the long-term land cover changes from 1986 to 2015, which shows a significant decrease in bare land which could be attributed to erosion due e.g., to sand mining, mangrove logging and sea level rise (UNDP, 2006). Increase in vegetation over the same period could be related to increase agriculture practises (UN DESA, 2015; UNDP, 2006; UNEP, 2004) as a result of population increases in Liberia, see Fig. 4.

Considering the constant complaint about deforestation through illegal logging in Liberia (Liberia, 2016; Siakor, 2014), it is quite surprising that the vegetation areas increased by 2.51% in size for the second period (1998–2002). During that time, Charles Taylor's regime, which started in 1997 exacerbated illegal logging to finance the conflict in Sierra Leone (Bowcott, 2013; Dick, 2003; Liberia, 2016). According to Fig. 3, although vegetation was changing into residential and bare land significantly near Monrovia coastline (Liberia's capital) over that period, the bare land areas (not in coastal area) were transformed into vegetation areas. This made the most contribution to vegetation increase possibly due to the fact that people were moving to inland areas in order to avoid the second civil war (1999–2003) thus converting bare land into agricultural land UNEP (2004). One of the evidence is that in 2015 (see Fig. 3), the inland area converted to built up areas (specially for the major cities in the study area). On the other hand, our study shows that the forested areas are not separated from vegetation class. The result of vegetation increment, therefore, is not entirely associated with forests, e.g., forests decreased but grass and agricultural land increased more. In the third period (2002–2015), vegetation started to decrease, what could be attributed to unregulated mining (UNDP, 2006) and illegal mangrove logging in the forested areas, see e.g., Mancini et al. (2013); UNDP (2006); Wiles (2005).

Regarding the residential increase near coastline regions during the second period (1998–2002), a probable explanation could be the fact that Charles Taylor took power during this period and advanced settlement. Figure. 3 could suggest that after the resignation of Charles Taylor in 2003, the end of Liberia's second civil war, lots of residential areas were abandoned and became uninhabited areas (Wiles, 2005). Secondly, a constant decrease in the bare land class over the evaluated years is a result of residential development as bare lands were turned into dwellings and agricultural lands (UNDP, 2006). As for the sediment, it almost disappeared after the civil war possibly be due to population increase in coastal regions as these areas were converted into new settlements, and also due to sand mining (UNDP, 2006). Water bodies did not vary so much in the first two periods (1986–2002), but increased during the third period (2002–2015), possibly due to coastal erosion attributed to mangrove logging, sand mining and sea level rise (El-Hattab, 2016; Wiles, 2005).

Liberia faced internal displacements during the civil wars where many residents migrated from rural to urban areas. In addition, the population increased in the 1970s from 1,500,000 to reach 4,859,221 persons in 2018 (Fig. 4). For example, Monrovia experienced a population increase over the period 1960 to 2018, i.e., from 80,000 to over 1,100,000 (UN DESA, 2015). This population increase in Monrovia could be explained by the fact that when the city was under the control of peace keeping forces and governed by interim governments, many internally displaced rural residents flocked in to seek shelter (see, e.g., UN DESA (2015)). This increase in population led to the expansion of the residential class by 1.43% and a decline in bare land by about 5.07% over the period 1986–2015 shown in Table 3.

4.2. Coastal analysis (1986–2015)

Two coastal change analyses are carried out on the coastal areas to quantify the areas of erosion, accretion and coastal shifts for the period 1986–2015. The results for the areas of erosion and accretion are shown in Fig. 5 and their average coastal shifts either erosion or accretion in Table 4. The period 1986–1998 exhibited more instances of accretion than erosion for the three regions namely; central, eastern and western, with an overall accretion of 66.7% and erosion of 32.0% for the entire study area (see Fig. 5). During this period, the increase in sediment

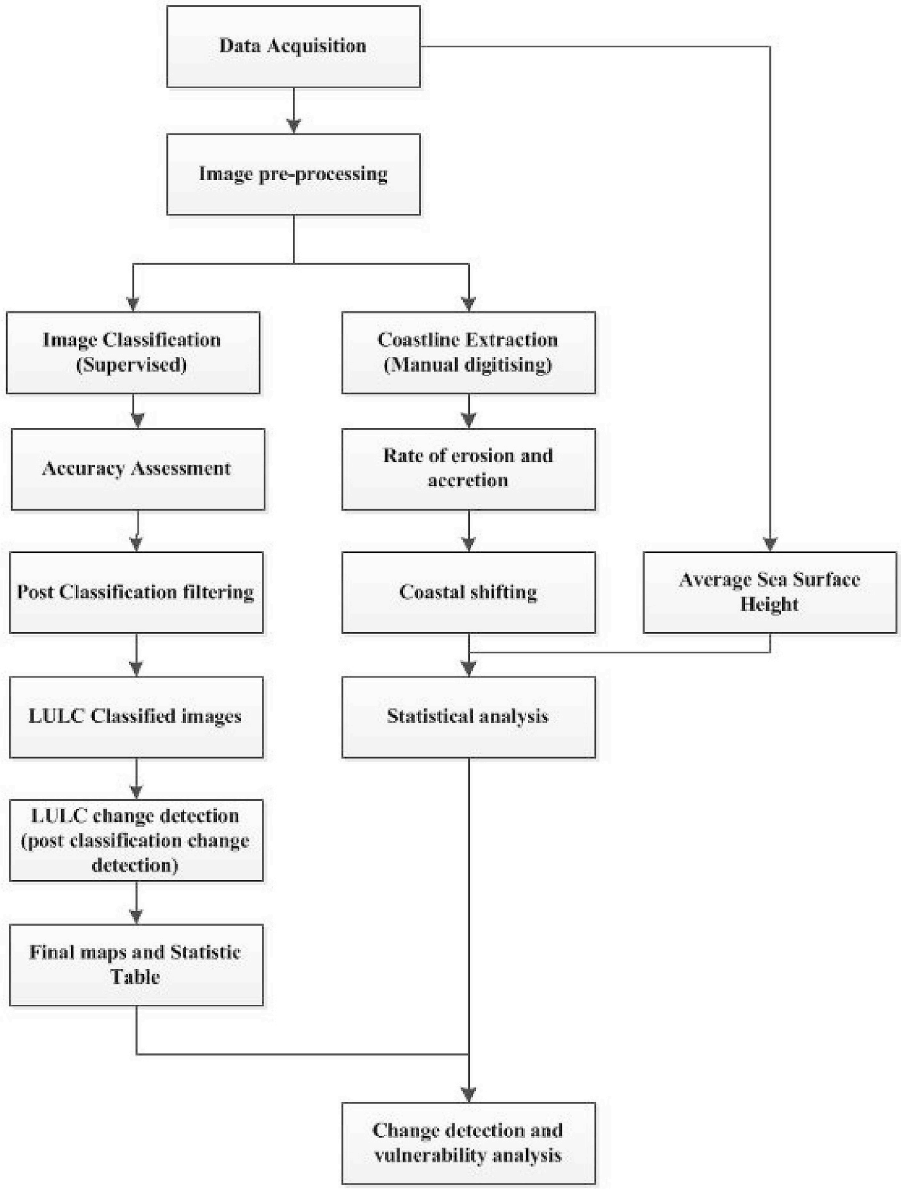

Fig. 2. A flowchart depicting the method, which entails of four steps; (i) data acquisition from USGS and CMEMS, (ii) raw datasets pre-processed to make them ready for data processing and analysis, (iii) data extraction and (iv) change detection and vulnerability analysis.

Table 2
Result for accuracy assessment, (C) = Classification data (unchanged areas for all classified images) and (R) = Reference data (Sentinel-2 2015), PA= Producer's accuracy, OA= Overall accuracy, KC= Kappa coefficient, and UA= User accuracy.

	Veg. (R)	Res. (R)	Wat. (R)	Bar. (R)	Sed. (R)	Sum	UA (%)
Vegetation (C)	88	5	5	0	0	98	90
Residential (C)	10	90	0	10	5	115	78
Water (C)	2	0	85	0	0	87	98
Bare land (C)	0	5	0	85	15	105	81
Sediment (C)	0	0	10	5	80	95	84
Sum	100	100	100	100	100	500	
PA (%)	88	90	85	85	80		
OA (%)	86						
KC	0.82						

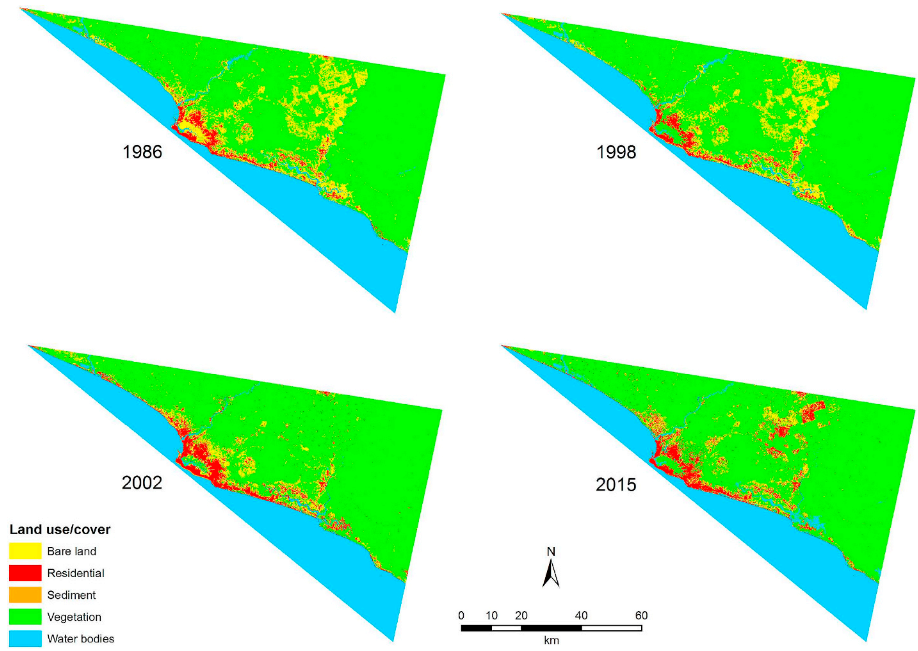

Fig. 3. LULC maps for the Liberian coastal regions (1986–2015) showing different land cover classes defined through classification. The dominant land cover class is the vegetation followed by water bodies and bare land.

Table 3
(a) Land use/cover (LULC) classes in percentage, and (b) their changes in percentage from 1986 to 2015.

(a) LULC class (%)	1986	1998	2002	2015
Bare land	10.63	9.58	5.91	5.57
Residential	2.45	2.40	3.64	3.88
Sediment	0.18	0.26	0.21	0.12
Vegetation	59.39	60.48	62.99	62.68
Water	27.35	27.28	27.25	27.76
(b) LULC change (%)	**1986–1998**	**1998–2002**	**2002–2015**	**1986–2015**
Bare land	−1.05	−3.67	−0.35	−5.07
Residential	−0.05	1.24	0.24	1.43
Sediment	0.07	−0.05	−0.09	−0.06
Vegetation	1.09	2.51	−0.31	3.29
Water	−0.06	−0.04	0.51	0.41

areas and the decrease in water surface areas along the coastal zones are the main reasons for this accretion, see Table 3. During the second period (1986–2002), which includes the post-war period, there was an erosion of about 85.2% in the entire study area. A total of 39.0% of areas were eroded in the central region while 36.1% and 10.1% of eroded areas are found in the eastern and western regions, respectively. This erosion is aligned with a study conducted by United Nation Development Programme (UNDP) in 2006, which show that the mangrove areas were degraded due to illegal logging, urban expansion, and unregulated sand mining (UNDP, 2006). For the last assessment period 1986–2015, the study area experienced more erosion than accretion (Fig. 5) with total areas of 64.8% and 33.6%, respectively. Again this eroded areas is a result of sand mining (UNDP, 2006; Wiles, 2005), and possible sea level rise by one metre in the coastal zone of Liberia, which was predicted for this century by Wiles (2005).

As already mentioned, coastal erosion can be caused by different factors including climate change and anthropogenic influences. The

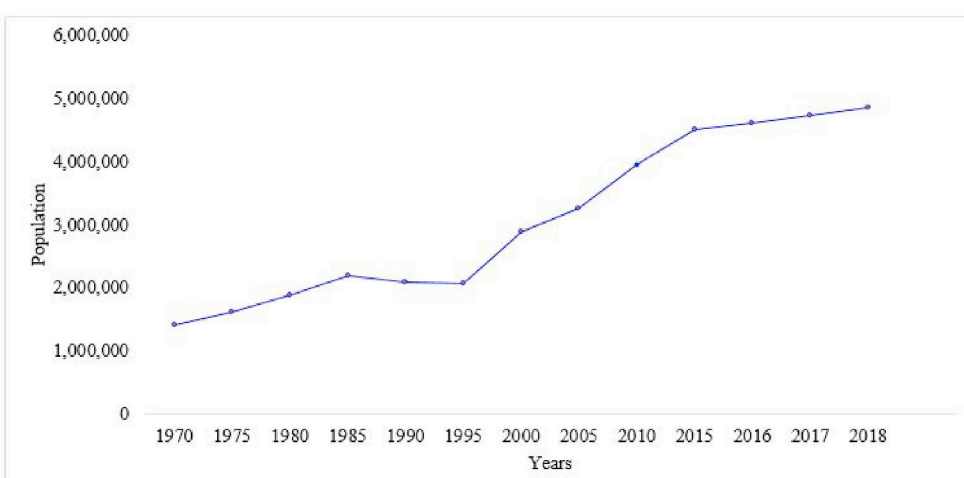

Fig. 4. Population trends of Liberia from 1970 to 2015. The data used were obtained from http://www.worldometers.info/world-population/liberia-population/.

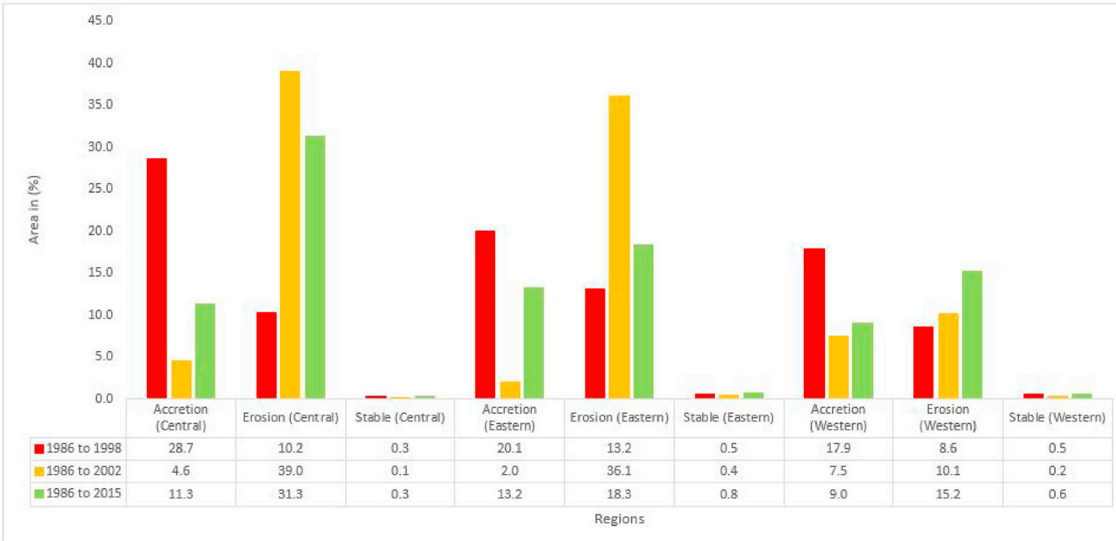

Fig. 5. Erosion and accretion in different sections of the study area for the three different periods assessed from 1986. The figure shows most instances of erosion in the second period (1986–2002).

Table 4
Average coastline shifting in (m) and their annual shift rates in (m/year) for the three regions during the study periods.

Coastal Status	1986 to 1998	1986 to 2002	1986 to 2015
Accretion (Central)	43.7 (3.6)	30.5 (1.9)	41.5 (1.4)
Accretion (Eastern)	43.7 (3.6)	30.7 (1.9)	104.8 (3.6)
Accretion (Western)	38.9 (3.2)	53.1 (3.3)	78.0 (2.7)
Erosion (Central)	−63.9 (−5.3)	−66.2 (−4.1)	−67.7 (−2.3)
Erosion (Eastern)	−74.7 (−6.2)	−76.0 (−4.8)	−50.1 (−1.7)
Erosion (Western)	−41.6 (−3.5)	−27.3 (−1.7)	−49.3 (−1.7)

observation from the United Nations Environment Programme (UNEP) 2004 study indicates that erosion along the coast of Liberia could be attributed to anthropogenic factors, i.e., unregulated destruction of coastal forests for fuelwood and sand mining (UNEP, 2004). More coastal erosion are observed during the period of increase in population, considering post-civil war. Other than the anthropogenic influences, climatic factors seem also to be contributing to coastal changes (UNDP, 2006; UNEP, 2004; Wiles, 2005). This is evidence by the statistical relationship found between increased instances of coastline erosion in the period considered and the increasing trends of sea level rise, see Fig. 8.

The coastal movement for the three regions (western, central, and eastern) are presented in Fig. 6, where the variation in coastline movement is slightly different for each region. The variability is less defined for the first period (1986–1998) than it is for the second (1986–2002) and third periods (1986–2015). The Eastern region seems to be shifting rather slowly compared to the other regions with the most notable variation happening between transect numbers 257 and 265 (Fig. 6). The coastal shift (either erosion or accretion) in Liberia is a result of many factors, i.e., sea level rise, since the coastal zones are common areas for flooding because of the rivers and estuary activities (Wiles, 2005). As mentioned before, erosion is a result of many factors, i.e., sand mining and sea level rise (UNDP, 2006) while accretion is mainly related to increases in bare land and sediments areas caused by illegal logging including mangrove in the coastal zones of Liberia (Wiles, 2005).

On average, the central region shifted (accretion) by 43.7, 30.5, and 41.5 m with annual shift rates of 3.6, 1.9 and 1.4 m/y for the three

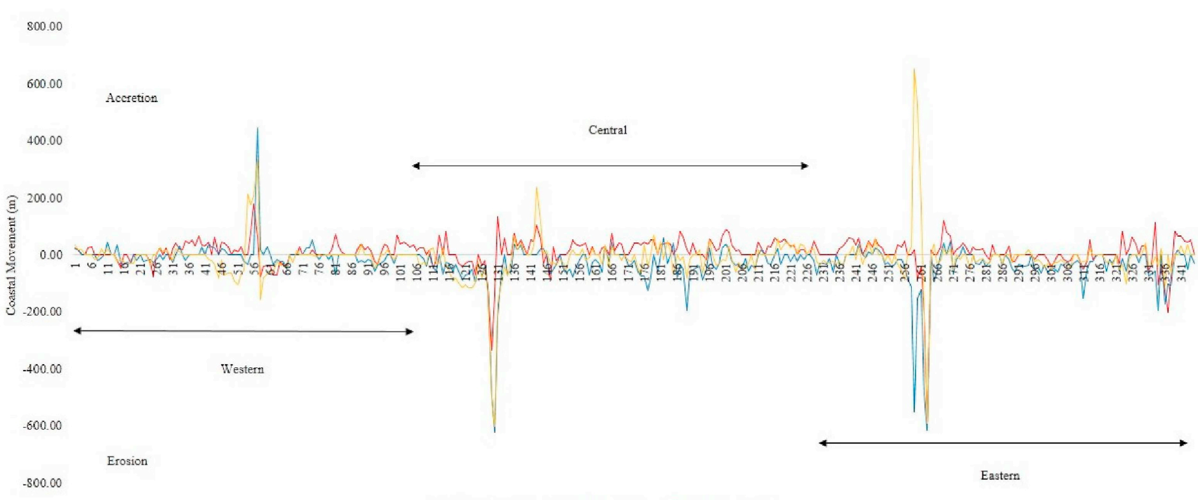

Fig. 6. Liberia's coastal shift analysis using transects with 500 m interval for Liberian's coastline from 1986 to 2015.

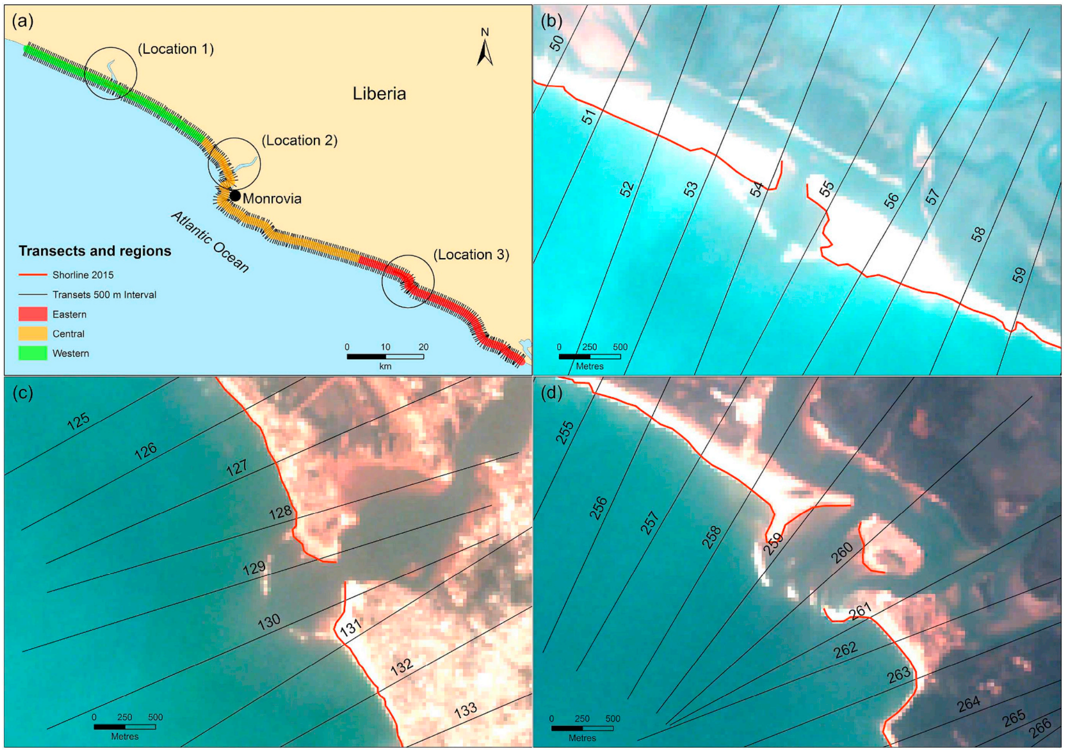

Fig. 7. Rivers and Estuaries influence along the Liberian shoreline (a) transects and regions, (b) location 1, (c) location 2, and (d) location 3.

periods (1986–1998, 1986–2002, and 1986–2015), respectively; the eastern region by 43.7, 30.7 and 104.8 m with annual shift rates of 3.6, 1.9 and 3.6 m/y, respectively and the western region by 38.9, 53.1, and 78.0 m, with annual shift rates of 3.2, 3.3 and 2.7 m/y, respectively (see Table 4). As for the erosion of the three regions, the central and eastern regions eroded more than the western region probably due to the impacts of climate change, i.e., sea level rise (predicted to rise by almost 1 m this century; (UNDP, 2006; Wiles, 2005)). Also, other factors such as mangrove logging and sand mining contributed to this erosion (i.e., 4.1 m/y and 4.8 m/y for the central and eastern regions, respectively),

Table 5
Coastal vulnerability status, where V1 = accretion, V2 = erosion, V3 = residential, V4 = vegetation and V5 = coastal slope. These are the vulnerability assessment variables used in this study.

Regions	V1	V2	V3	V4	V5	Final score
Central	very low	very high	very low	very low	high	very low
Eastern	very low	very high	very high	very low	high	very high
Western	very low	very high	moderate	very low	high	high

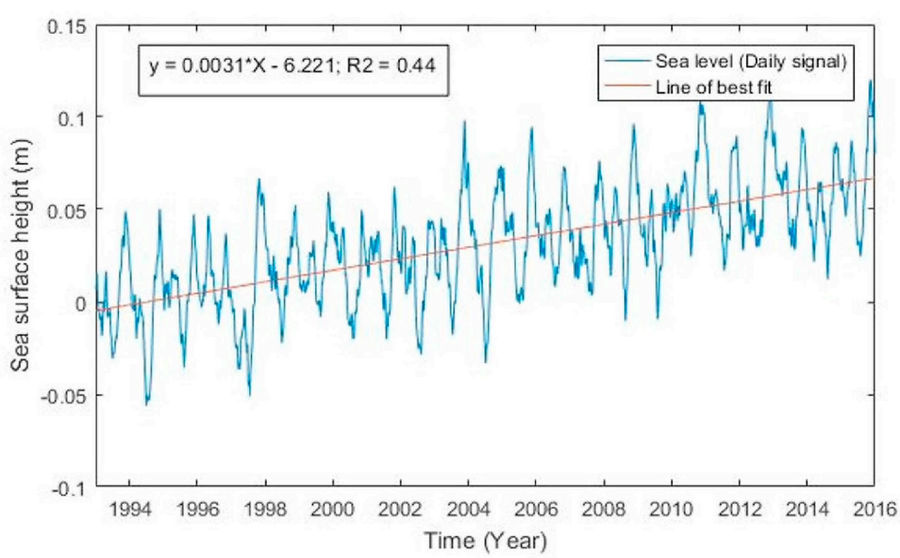

Fig. 8. Sea surface variability in Liberia. The graph represents the daily sea surface heights from 1993 to 2015.

for the period 1986–2002. Our results thus align very well with the 3–4 m/y erosion rates estimated by UNEP (2004) for the 1986–2001 period.

Although climate change is thought to be the main contributor to the coastal zone erosion through e.g., sea level rise, there could however be other factors. UNDP (2006) presents unregulated mining, coastal sand mining, and rivers and estuaries activities along the coastal zone of Liberia as being contributors to Liberia's coastal erosion. For instance, Fig. 7 represents the rivers and estuaries along the shoreline of Liberia, which may have high influence on coastal dynamics, i.e., erosion or accretion. This observation was visible clearly in Fig. 6 through the orthogonal transects analysis, which have experienced higher shifting, i.e., accretion for the western region, erosion for the central region, and both accretion and erosion for the eastern region. These three locations (Fig. 7 (a)) are represented in more details with the transacts numbers in Fig. 7 (b), (c) and (d), respectively. The rivers and estuaries' flooding and sediment transport have local influences on the coastline positional status during the evaluated years in this study (UNDP, 2006; UNEP, 2004; Wiles, 2005).

4.3. Coastline changes and vulnerability assessment

From the coastline vulnerability assessment presented in Table 5, the central region is shown to be very low in terms of vulnerability to erosion with three out of all indicator variables falling under very low vulnerability category. The western region shows a high vulnerability status whereas the eastern region shows very high vulnerability to erosion. The results are somehow counter-intuitive. The central region, which eroded more than the western region and almost at the same rate with eastern is shown as being very lowly vulnerable to erosion. During the vulnerability assessment, the threshold value for residential was determined based on the apparent positive correlation it has with the erosion. Evidently, that played a role in understanding the vulnerability of coastal regions studied. The erosion and accretion patterns in most of the cases for this study matched with LULC classes changes. The water and sediment classes, for example, have increased and decreased respectively in periods where there was more erosion than accretion, see Table 3. As water moves and encroaches the beach, there is seemingly an increase in the water areas and a commensurate decrease in beach sand or sand dunes. Intuitively, the most populated coastal regions, i.e., the central region, should be the most vulnerable to coastal erosion. From erosion and accretion study, periods of increased population coincided with more erosion and this associated with increase in residential areas (a positive correlation was found between erosion and residential, see Fig. 9). The increase in population resulted in an increase of sand mining and mangrove logging by local residents in coastal zones of Liberia (UNDP, 2006). The Eastern region, which includes Harbel, the 7th most populated city in Liberia (City population, 2008) showed a relatively higher erosion during the post-war period.

The erosion of 85.2% in the study area during the post-war era (1986–2002) is quite a big increase from the previous period (1986–1998), which was predominantly the period of the civil war. As already stated, this increase in erosion for the coastal zone are a result of mangrove logging and sand mining in these areas, see, e.g., UNEP (2004); Wiles (2005); UNDP (2006). The period between 1986 and 2015, includes a period of both civil war and post-civil war. The second civil war started around 2000 and people started fleeing the country in large numbers in 2002. This second civil war ended in 2003 but people started to return to the country again in 2005 after the election (CDC, 2017). Erosion of 64.8% during this period, is considerably less than during the period 1986–2002. Based on the erosion and accretion patterns observed throughout the study, it is evident that the variables, which have been used during the coastline vulnerability mapping and assessment were sufficient indicators.

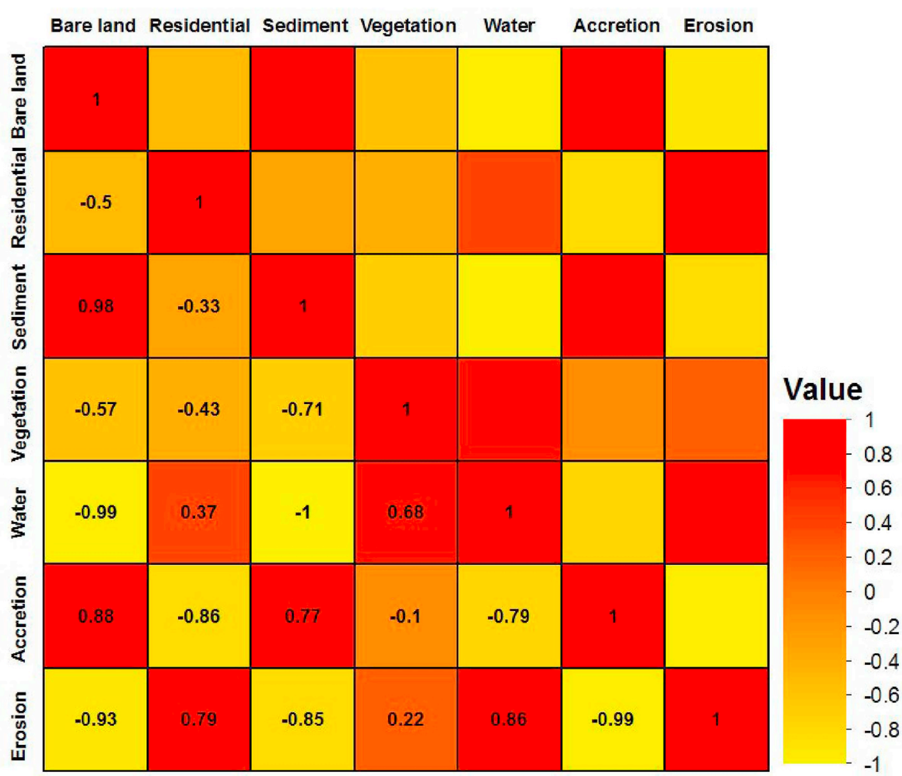

Fig. 9. Correlation coefficients. The variables in the first five rows are the LULC classes (Bare land, Residential, Sediment, Vegetation and Water) followed by accretion and erosion. These values are statistically significant at 95% confidence level for erosion, sediment, and residential (*p-value*<0.05).

Table 6
Estimated slopes for both sea level anomaly and coastline shifting and their respective descriptive statistics. The hypothesis test results are also shown.

	Sea level	Coastline shifting	Test statistic values
Sample size	345	8401	
Slope	−1.256	0.003	
Mean	−12.146	0.031	
Variance	7271.953	0.001	
Standard deviation	85.276	0.031	
t'			0.27
Critical t - value			1.97
Degree of freedom			344
Significant level			0.05

4.4. Sea level changes

Liberia's sea level change time series derived from multi-mission satellite altimetry is presented in Fig. 8, which shows an increasing pattern in the sea level over the period 1993–2015. This is evident by the slopes of 0.0031 m, which is roughly an increase of 0.72 m for the 22 year period considered. Wiles (2005) predicted that global warming will be accompanied by a rise in sea levels over this century for Liberia by as much as 60–100 cm and could results in the subsidence of low-lying coastal areas. This prediction is aligned with the sea level changes derived from multi-mission satellite altimetry, which is presented in Fig. 8. Other than climate-induced sea level rise in Liberia (e.g., UNDP (2006); Wiles (2005)), other factors such as subsidence have also been reported as possible causes of sea level rise (see, e.g., Hinkel et al. (2012); Dasgupta, Laplante, Murray, and Wheeler (2009); Brown, Kebede, and Nicholls (2011)). Sea level rise, regardless of the source, could possibly lead to erosion along the Liberian coast as predicted by Wiles (2005).

4.5. Correlation and hypothesis testing

Fig. 9 shows the correlation analysis for bare land, residential, sediment, vegetation and water with accretion and erosion. Bare land is positively correlated with accretion (0.88) and sediment (0.98) as expected. On the other hand, this class is negatively correlated with erosion and water (i.e., −0.93 and −0.99, respectively). Also, the analysis indicate that the erosion process is strongly correlated with the residential settlement (0.79). This could be related to the fact that the built up areas increased beyond the shoreline of the study area as mapped and quantified in Fig. 3 and Table 3. On the other hand, the vegetation cover shows very weak correlation with erosion as expected because there were no vegetation cover present within coastal zones of Liberia after sand mining and mangrove logging process (UNDP, 2006; Wiles, 2005). However, Table 3 shows that the vegetation class is increasing possibly due to the fact that the entire study area and not only the coastal zone was considered for this analysis.

Table 6 shows the descriptive statistics for the two estimated slopes tested using the Welsh's t-test. The information in the table used Eq. (1) to derived t', which was tested against the critical t value using the degree of freedom (Eq (2)) at 0.05 significant level. The degree of freedom is given as 344, the computed Welsh's t' value is 0.27 and the critical t value is 1.97. Since the computed Welsh's t' is less than the critical t value, the null hypothesis that the two slopes are statistically similar is accepted implying that the increase in sea level and increase in erosion are statistically similar, further corroborating the findings of Wiles (2005) that the sea level rise in future could possibly lead to erosion along the Liberian coast.

5. Conclusions

The study assessed Liberia's LULC changes, coastal changes and vulnerability to erosion using Landsat data for the period 1986–2015. The most important findings of this study are:

- Liberia's coast experienced decrease in the sediment and bare land classes over the period 1986–2015. Water and residential classes experienced increase, which may be attributed to many factors, e.g., sea level rise, sand mining, mangrove logging and population increase. Vegetation cover on its part maintained the unchanged status above 59%.
- Erosion along the coast of Liberia could be attributed to anthropogenic factors. The level and rates of coastal erosion during the time of civil war is not as significant as during the post-civil war era. Furthermore, rivers and estuaries along the shoreline of Liberia as well as climate change, i.e., sea level rise as evidenced from the statistical relationship between increased instance of coastline erosion for the period considered and the increasing trend of sea level of changes could be contributing factors.
- For validation of Landsat data (30 m spatial resolution), Sentinel-2 MSL data, endowed with the advantage of moderate spatial resolution (10 m) is used. Sentinel data, which will be available over the next decade will be useful in providing reference data (when in-situ data collection is not possible). This will be useful for capturing the effects of human activities and others factors including climate change on coastal vulnerability (e.g., due to erosion).

References

Abd El-Kawy, O. R., Rød, J. K., Ismail, H. A., & Suliman, A. S. (2011). Land use and land cover change detection in the western Nile delta of Egypt using remote sensing data. *Applied Geography, 31*(2), 483–494. https://doi.org/10.1016/j.apgeog.2010.10.012.

Alesheikh, A. A., Ghorbanali, A., & Nouri, N. (2007). Coastline change detection using remote sensing. *International Journal of Environmental Science & Technology, 4*(1), 61–66. https://doi.org/10.1007/bf03325962.

Anderson, J. R. (1976). *A land use and land cover classification system for use with remote sensor data: Vol. 964*US Government Printing Office.

Appeaning Addo, K., Walkden, M., & Mills, J. P. (2008). Detection, measurement and prediction of shoreline recession in Accra, Ghana. *ISPRS Journal of Photogrammetry and Remote Sensing, 63*(5), 543–558. https://doi.org/10.1016/j.isprsjprs.2008.04.001.

Awange, J. L. (2012). *Environmental Monitoring Using GNSS. Global Navigation Satellite Systems.* Berlin, Heidelberge, New York: Springer-Verlaghttps://doi.org/10.1007/978-3-540-88256-5.

Awange, J. L. (2018). *GNSS Environmental Sensing. Revolutionizing Environmental Monitoring.* Springer International Publishing AGhttps://doi.org/10.1007/978-3-319-58418-8.

Awange, J., Forootan, E., Kusche, J., Kiema, J., Omondi, P., Heck, B., & Gonalves, R. (2013). Understanding the decline of water storage across the Ramser-Lake Naivasha using satellite-based methods. *Advances in Water Resources, 60*, 7–23.

Bowcott, O.. War criminal Charles taylor to serve 50-year sentence in British prison news paper the guardian. (2013). available on https://www.theguardian.com/world/2013/oct/10/former-liberian-president-charles-taylor-british-prison (October, 2016).

Brown, S., Kebede, A. S., & Nicholls, R. J. (2011). *Sea-level rise and impacts in Africa, 2000 to 2100.* UK: School of Civil Engineering and the Environment University of Southampton.

Bryan, B., Harvey, N., Belperio, T., & Bourman, B. (2001). Distributed process modeling for regional assessment of coastal vulnerability to sea-level rise. *Environmental Modeling & Assessment, 6*(1), 57–65.

CDC (2017). *2014 Ebola outbreak in West Africa - case counts.* Centers for Disease Control and Prevention. Retrieved 17 July, 2017, from https://www.cdc.gov/vhf/ebola/outbreaks/2014-west-africa/case-counts.html.

Cihlar, J. (2000). Land cover mapping of large areas from satellites: Status and research priorities. *International Journal of Remote Sensing, 21*, 1093–1114.

City population. Republic of Liberia. (2008). available on https://www.citypopulation.de/Liberia.html (November, 2016).

Dasgupta, S., Laplante, B., Murray, S., & Wheeler, D. (2009). *Climate change and the future impacts of storm-surge disasters in developing countries*.

Dewan, A., Corner, R., Saleem, A., Rahman, M. M., Haider, M. R., Rahman, M. M., et al. (2017). Assessing channel changes of the Ganges-Padma River system in Bangladesh using Landsat and hydrological data. *Geomorphology, 276*, 257–279. https://doi.org/10.1016/j.geomorph.2016.10.017.

Dewan, A. M., & Yamaguchi, Y. (2009). Land use and land cover change in Greater Dhaka, Bangladesh: Using remote sensing to promote sustainable urbanization. *Applied Geography, 29*, 390–401. https://doi.org/10.1016/j.apgeog.2008.12.005.

Dick, S. (2003). *Liberia.* FMO. available on http://www.forcedmigration.org/research-resources/expert-guides/liberia/alldocuments (October, 2016) .

Drusch, M., Del Bello, U., Carlier, S., Colin, O., Fernandez, V., Gascon, F., et al. (2012). Sentinel-2: ESA's optical high-resolution mission for GMES operational services.

Remote Sensing of Environment, 120, 25–36.
El-Hattab, M. M. (2016). Applying post classification change detection technique to monitor an Egyptian coastal zone (Abu Qir bay). *The Egyptian Journal of Remote Sensing and Space Science, 19*, 23–36. https://doi.org/10.1016/j.ejrs.2016.02.002.
ESA (2017). *European space agency, copernicus open access Hub*. SERCO.
Gilmore, S., Saleem, A., & Dewan, A. (2015). *Effectiveness of DOS (Dark-Object Subtraction) method and water index techniques to map wetlands in a rapidly urbanising megacity with Landsat 8 data.* In Research@ Locate'15100–108. http://SunSITE.Informatik.RWTH-Aachen.DE/Publications/CEUR-WS/.
Global Environmental Facility. LDCF - Liberia - enhancing resilience of vulnerable coastal areas to climate change risks. (2010). Available on: https://www.thegef.org/news/ldcf-liberia-enhancing-resilience-vulnerable-coastal-areas-climate-change-risks (November, 2016) .
Goncalves, R. M., & Awange, J. L. (2017). Three Most Widely Used GNSS-Based Shoreline Monitoring Methods to Support Integrated Coastal Zone Management Policies. *Journal of Surveying Engineering, 143*(3), 05017003.
Goncalves, R. M., Awange, J., & Krueger, C. P. (2012a). GNSS-based monitoring and mapping of shoreline position in support of planning and management of Matinhos/PR (Brazil). *Journal of Global Positioning Systems, 11*(1), 156–168.
Goncalves, R. M., Awange, J., Krueger, C. P., Heck, B., & Coelho, L. S. (2012b). A comparison between three short-term shoreline prediction models. *Ocean & Coastal Management, 69*, 102–110. https://doi.org/10.1016/j.ocecoaman.2012.07.024.
González-Sanpedro, M., Le Toan, T., Moreno, J., Kergoat, L., & Rubio, E. (2008). Seasonal variations of leaf area index of agricultural fields retrieved from Landsat data. *Remote Sensing of Environment, 112*, 810–824.
Graham, K. (2014). Liberia's losing battle with erosion and rising sea levels. *Environment*. available on http://www.digitaljournal.com/news/environment/liberia-s-losing-battle-with-erosion-and-rising-sea-levels/article/392869 (November, 2016) .
Hinkel, J., Brown, S., Exner, L., Nicholls, R. J., Vafeidis, A. T., & Kebede, A. S. (2012). sea-level rise impacts on Africa and the effects of mitigation and adaptation: An application of DIVA. *Regional Environmental Change, 12*(1), 207–224.
Jayson-Quashigah, P.-N., Addo, K. A., & Kodzo, K. S. (2013). Medium resolution satellite imagery as a tool for monitoring shoreline change. Case study of the Eastern coast of Ghana. *Journal of Coastal Research, 65*, 511–516. https://doi.org/10.2112/si65-087.1.
Jensen, J. R., Rutchey, K., Koch, M. S., & Narumalani, S. (1995). Inland wetland change detection in the Everglades Water Conservation Area 2A using a time series of normalized remotely sensed data. *Photogrammetric Engineering and Remote Sensing, 61*, 199–209.
John, P. (2017). *Globalsecurityorg.* Retrieved 17 July, 2017, from http://www.globalsecurity.org/military/world/war/liberia-1997.htm.
Jusoff, K., & Senthavy, S. (2003). Land use change detection using remote sensing and geographical information system (GIS) in Gua Musang district, Kelantan, Malaysia. *Journal of Tropical Forest Science, 15*, 303–312.
Kauth, R., Lambeck, P., Richardson, W., Thomas, G., & Pentland, A. (1979). *Feature extraction applied to agricultural crops as seen by Landsat*.
Kesgin, B., & Nurlu, E. (2009). Land cover changes on the coastal zone of Candarli Bay, Turkey using remotely sensed data. *Environmental Monitoring and Assessment, 157*, 89–96.
Liberia. Countries. (2016). available on http://www.illegal-logging.info/regions/liberia (November, 2016).
LISGIS (2014). *Liberia demographic and health survey 2013.* available on https://dhsprogram.com/pubs/pdf/FR291/FR291.pdf (November, 2016) .
MacDougall, C. (2016). *Fearing the tide in West Point, a slum already swamped with worry, news paper article.* The New York Times. available on http://www.nytimes.com/2016/03/16/world/africa/fearing-the-tide-in-west-point-a-slum-already-swamped-with-worry.html?_r=0 (November, 2016) .
Mancini, F., Dubbini, M., Gattelli, M., Stecchi, F., Fabbri, S., & Gabbianelli, G. (2013). Using unmanned aerial vehicles (UAV) for high-resolution reconstruction of topography: The structure from motion approach on coastal environments. *Remote Sensing, 5*(12), 6880–6898.
Mather, P. M., & Koch, M. (2011). *Computer processing of remotely-sensed images: An introduction* (4 ed.). Chichester, West Sussex: UK Wiley-Blackwell.
Mendonça, F. J. B., Gonclaves, R. M., Awange, J., Silva, L. M. d., & Gregorio, M. d. N. (2014). Temporal shoreline series analysis using GNSS. *Boletim de Ciências Geodsicas, 20*(3), 701–719.
Misra, A., & Balaji, R. (2015). A study on the shoreline changes and LAND-use/land-cover along the south Gujarat coastline. *Procedia Engineering, 116*, 381–389. https://doi.org/10.1016/j.proeng.2015.08.311.
Moran, E. F. (2010). Land cover classification in a complex urban-rural landscape with QuickBird imagery. *Photogrammetric Engineering and Remote Sensing, 76*, 1159.
Moser, B. K., Stevens, G. R., & Watts, C. L. (1989). The two-sample t-test versus Satterthwaite's approximate F test. *Communications in Statistics-theory and Methods, 18*(11), 3963–3975.
Nicholls, R. J., & Cazenave, A. (2010). Sea-level rise and its impact on coastal zones. *Science, 328*(5985), 1517–1520. https://doi.org/10.1126/science.1185782.
Otukei, J. R., & Blaschke, T. (2010). Land cover change assessment using decision trees, support vector machines and maximum likelihood classification algorithms. *International Journal of Applied Earth Observation and Geoinformation, 12*, S27–S31.
Pardo-Pascual, J. E., Almonacid-Caballer, J., Ruiz, L. A., & Palomar-Vzquez, J. (2012). Automatic extraction of shorelines from Landsat TM and ETM+ multi-temporal images with subpixel precision. *Remote Sensing of Environment, 123*, 1–11. https://doi.org/10.1016/j.rse.2012.02.024.
Parrish, C. E., Sault, M., White, S. A., & Sellars, J. (2005). Empirical analysis of aerial camera filters for shoreline mapping. *Proceedings of the american society for photogrammetry and remote sensing annual conference, Baltimore, Maryland* (pp. 1–11). .
Pendleton, E. A., Thieler, E. R., & Williams, S. J.. Coastal vulnerability assessment of golden gate national recreation area to sea-level rise. (2005). available on http://pubs.usgs.gov/of/2005/1058/images/pdf/report.pdf (September, 2016).
Peterson, U., & Aunap, R. (1998). Changes in agricultural land use in Estonia in the 1990s detected with multitemporal Landsat MSS imagery. *Landscape and Urban Planning, 41*, 193–201.
Poornima, K. V., & Chinthaparthi, S. (2014). Detection and future prediction of coastal changes in Chennai using remote sensing and GIS techniques. *International Journal of Innovative Research in Science, Engineering and Technology, 3*(2), 9456–9462.
Porter-Bolland, L., Ellis, E. A., & Gholz, H. L. (2007). Land use dynamics and landscape history in La Montaña, Campeche, Mexico. *Landscape and Urban Planning, 82*, 198–207.
Rawat, J. S., & Kumar, M. (2015). Monitoring land use/cover change using remote sensing and GIS techniques: A case study of Hawalbagh block, district Almora, Uttarakhand, India. *The Egyptian Journal of Remote Sensing and Space Science, 18*(1), 77–84. https://doi.org/10.1016/j.ejrs.2015.02.002.
Ruxton, G. D. (2006). The unequal variance t-test is an underused alternative to Student's t-test and the Mann–Whitney U test. *Behavioral Ecology, 17*(4), 688–690.
Saleem, A., Corner, R., & Awange, J. (2018). On the possibility of using CORONA and Landsat data for evaluating and mapping long-term LULC: Case study of Iraqi Kurdistan. *Applied Geography, 90*, 145–154.
Salghuna, N., & Bharathvaj, S. A. (2015). Shoreline change analysis for northern part of the coromandel coast. *Aquatic Procedia, 4*, 317–324.
Siakor, S. K. A. (2014). *Illegal logging persists in Liberia, News paper.* Pambazuka News. available on http://www.pambazuka.org/printpdf/89095 (November, 2016) .
Smith, J. T., Jr. (1981). *A history of flying and photography in the photogrammetry division of the national ocean survey, 1919-79.* Silver springMaryland: U.S. Department of Commerce, National Oceanic and Atmospheric Administration, National Ocean Service.
Song, C., Woodcock, C. E., Seto, K. C., Lenney, M. P., & Macomber, S. A. (2001). Classification and change detection using Landsat TM data: When and how to correct atmospheric effects? *Remote Sensing of Environment, 75*(2), 230–244.
Sousa, P. H. G. O., Siegle, E., & Tessler, M. G. (2013). Vulnerability assessment of massaguaçú beach (SE Brazil). *Ocean & Coastal Management, 77*, 24–30. https://doi.org/10.1016/j.ocecoaman.2012.03.003.
Stow, D., Tinney, L., & Estes, J. (1980). *Deriving land use/land cover change statistics from Landsat-A study of prime agricultural land*.
The World Bank. Liberia IBRD.IDA. (2016). Available on http://www.worldbank.org/en/country/liberia (November, 2016).
UN DESA. World population prospects 2015. (2015). Available on https://esa.un.org/unpd/wpp/ (October, 2016).
UNDP. First State of the environment report for Liberia - 2006. (2006). https://www.thegef.org/sites/default/files/ncsa-documents/State_of_the_environment_report_final.pdf (August, 2018).
UNDP. The republic of Liberia: Enhancing the resilience of vulnerable coastal areas to climate change risks. (2015). Available on http://adaptation-undp.org/sites/default/files/downloads/brief_3975_liberia.pdf (September, 2016).
UNEP (2004). *Desk study on the environment in Liberia.* Geneva: United Nations Environment Programme. https://postconflict.unep.ch/publications/Liberia_DS.pdf (August, 2018).
USAID. Climate change adaptation in Liberia. (2012). available on https://www.climatelinks.org/sites/default/files/asset/document/liberia_adaptation_fact_sheet_jan2012.pdf (October, 2016).
USGS (2015). *Landsat data.* United States: USGS.
Vittek, M., Brink, A., Donnay, F., Simonetti, D., & Descle, B. (2014). Land cover change monitoring using Landsat MSS/TM satellite image data over West Africa between 1975 and 1990. *Remote Sensing, 6*, 658–676.
Werrell, C., & Femia, F. (2014). *Liberias rising waters.* Climate and Security, available on https://climateandsecurity.org/2014/08/19/liberias-rising-waters/ (November, 2016) .
Wiles, D. (2005). Coastal zone vulnerability and adaptation to climate change in Liberia. *Paper presented at the training workshop on adaptation and vulnerability to climate change, Maputo, Mozambique*.
Williams, W. C. L. (2016). *Liberias poor and the rising sea.* Inter Press Service. available on http://www.ipsnews.net/2014/06/liberias-poor-and-the-rising-sea/ (November, 2016) .
Yadav, P., Kapoor, M., & Sarma, K. (2012). Land use land cover mapping, change detection and conflict analysis of Nagzira-Navegaon corridor, Central India using geospatial technology. *International Journal of Remote Sensing and GIS, 1*, 90–98.
Yu, K., Hu, C., Muller-Karger, F. E., Lu, D., & Soto, I. (2011). Shoreline changes in west-central Florida between 1987 and 2008 from Landsat observations. *International Journal of Remote Sensing, 32*(23), 8299–8313. https://doi.org/10.1080/01431161.2010.535045.

Further reading

Munive, J. (2013). Liberia: Local politics, state-building and reintegration of populations. *States of Fragility, 43*, 12–14.